PAPER

Check for updates

Fabrication of microcapsules encapsulating *L. rhamnosus* GG with Eudragit® L100–trehalose and polysaccharides: a study on physicochemical properties and cell adhesion

Yuyan Xu,[ab] Shuangying Zhu, [ID] [b] Xinyi Sun,[b] Kai Shan,[b] Chong Zhang,[b] Hongmei Xiao,[ab] Xia Fan[b] and Chuang Zhang*[ab]

Our previous study revealed the relationship between the droplet-to-particle transition process and the functionality of *Lacticaseibacillus rhamnosus* GG (LGG) particles encapsulated with Eudragit® L100 (L100)–trehalose (Tre). The main focus was on exploring the effects of convective drying conditions on the targeted delivery of viable bacteria to the intestine, by using a single droplet drying technique to mimic realistic spray drying conditions. In the current study, spray-dried L100–Tre–LGG microcapsules combined with polysaccharides (maltodextrin, inulin, and soluble soy polysaccharides) were fabricated, to investigate the physicochemical properties of powders and the adhesion ability of spray-dried LGG cells. The results showed that L100–Tre powder exhibited better moisture content (4.84%) and hygroscopicity (17.94%) than the other three powders produced with L100–Tre and polysaccharides. Moreover, the LGG in the powders retained a high viability of 9 log CFU g^{-1} after spray drying and maintained 7 log CFU g^{-1} after 8 weeks of storage. Notably, all powders exhibited desirable survival rates of 87.4–93% for LGG after *in vitro* digestion. In addition, spray drying had minimal impact on the cell adhesion ability of LGG, maintaining an adhesion rate of 80% to Caco-2 cells. The L100–Tre–LGG probiotic spray-dried powders exhibit long shelf stability and strong adhesion capacity, providing strong support for the industrial production of probiotic products.

Sustainability spotlight

Global food systems face challenges of low probiotic viability and high energy consumption. Our L100–trehalose–polysaccharide microencapsulation system for *Lacticaseibacillus rhamnosus* GG achieves high viability and intestinal adhesion, reducing dosage requirements and manufacturing waste. Innovations include optimized drying for energy efficiency, improved gastrointestinal survival to minimize waste, and the use of biodegradable materials. Aligned with UN Sustainable Development Goals, this system enhances nutrition and health through stable probiotics, reduces carbon emissions, and extends shelf life, advancing sustainable functional food production.

1. Introduction

Probiotics are defined as "live microorganisms which, when administered in adequate amounts, confer a health benefit on the host".[1] The concept of the microbiota–brain–gut axis has gained significant recognition, highlighting the importance of successfully delivering probiotics to the intestine to reconstruct the intestinal microenvironment. The gut microbiota communicates with the brain through multiple pathways, including the immune system, tryptophan metabolism, the vagus nerve, and the enteric nervous system.[2] For example, short-chain fatty acids (SCFAs), such as butyric acid produced by fermentation of dietary fiber by intestinal microbes, can cross the blood–brain barrier, modulate microglial activity (the brain's resident immune cells), and affect neurodevelopment.[3] Oral administration of probiotic supplements has been shown to modulate the composition of the human gut microbiota. Certain probiotic strains, such as *Bifidobacterium bifidum*, lower intestinal pH by producing SCFAs, thereby creating a favorable environment for the growth of beneficial commensal bacteria, including *Faecalibacterium prausnitzii*.[4] In addition, probiotics help suppress pathogenic bacteria (*e.g.*, *Escherichia coli* and *Salmonella* spp.) through several mechanisms: (1) competitive exclusion by occupying mucosal adhesion sites, (2) competition for nutrients, and (3) secretion of antimicrobial compounds, such as bacteriocins, lactic acid, and hydrogen peroxide.[5]

ªSanya Research Institute, Nanjing Agricultural University, Sanya, Hainan 572025, China. E-mail: zhangchuang@njau.edu.cn

ᵇCollege of Food Science and Technology, Nanjing Agricultural University, Nanjing, Jiangsu 210095, China

Spray drying, known for its high efficiency and low energy consumption, has emerged as a preferred method for probiotic microencapsulation. Enhancing the quality of probiotic powder preparation is crucial to ensure that probiotics effectively participate in the human body's metabolic and immune processes. One critical factor is maintaining high viability of probiotics upon reaching the intestine. During spray drying, probiotic cells are exposed to heat, dehydration and oxidative stress, all of which can compromise cell integrity and lead to cell death.[6,7] Cellular components are particularly vulnerable: membrane damage occurs at about 50 °C, and the 30S ribosomal subunit is impaired at 60 °C, proteins begin to denature at 65 °C, and DNA damage becomes evident around 90 °C.[8] The removal of bound water further disrupts the stability of proteins, DNA, lipids, and overall cellular structure.[9] For instance, *L. helveticus* experiences significant loss of viability when the water content drops below around 0.3–0.5 g H_2O per g dry weight.[10] Beyond the drying process, probiotics are also subject to environmental stresses during storage and digestion.[11]

The physicochemical properties of the resulting probiotic powder, such as porosity, density and hygroscopicity, are critical in determining its protective capacity.[12] Notably, particle size and surface morphology (*e.g.*, hollowness or surface cracks) can significantly affect the effectiveness of microencapsulation.[13] Alvarado-Reveles *et al.*[14] reported that encapsulating *Lactobacillus rhamnosus* GG (LGG) in buttermilk proteins combined with agave fructans yielded particles with an average diameter of 52.4 μm, which improved bacterial survival by shielding against environmental and gastrointestinal stresses while enhancing bioaccessibility. Similarly, Chaikham *et al.*[15] found that increasing maltodextrin content to 20% reduced probiotic particle size and led to wrinkled surfaces, whereas a blend of 10% maltodextrin and 10% inulin produced larger, smoother particles. The mixed formulation also improved bacterial survival, retaining one log CFU g^{-1} more viable cells after spray drying compared to the maltodextrin-only system.

Selecting an appropriate wall material is crucial for protecting probiotics. Oligosaccharides such as trehalose (Tre) are well known for their protective role during spray drying, where they replace water molecules and help maintain cell membrane integrity.[16] However, oligosaccharides alone provide limited protection in the harsh gastric environment, rendering probiotics susceptible to acidic degradation and bile salt inactivation.[17] To overcome this limitation, the incorporation of Eudragit® L100 (L100), a pH-responsive polymer, offers a complementary solution.[18] Unlike Tre, L100 remains insoluble under acidic gastric conditions but dissolves at intestinal pH, allowing targeted probiotic release in the colon and minimizing inactivation in the stomach. Thus, the combination of Tre and L100 represents a promising strategy for developing an intestinal-targeted probiotic delivery system.

In our previous research, we found that the L100–Tre system could synergistically enhance the viability of probiotics after thermal convective drying. L100, adsorbed on the particle surfaces during evaporation, endowed the powder with intestinal-targeted delivery functions.[18] However, there was limited focus on the physiological functions of probiotics and

the physicochemical characteristics of the powder. Thus, this study aimed to analyse the physicochemical properties of L100–Tre–LGG particles, optimize the L100–Tre–LGG system, and investigate the physiological functions of microencapsulated probiotics. This study may provide new insights and references regarding the application of spray drying encapsulation in the delivery of probiotics and functional foods.

2. Materials and methods

2.1. Materials

The LGG strain (ATCC 53103) used in this study was obtained from our laboratory collection (College of Food Science and Technology, Nanjing Agricultural University, Nanjing, China). MRS broth powder and MRS agar powder were purchased from Hopebio Ltd (Qingdao, China). Eudragit® L100 (L100) was obtained from Evonik Industries AG (Shanghai, China). Trehalose was purchased from Sinopharm Chemical Reagent Co., Ltd (Shanghai, China). Maltodextrin was kindly provided as a gift by Ingredion Ltd (Shanghai, China). Inulin and soybean soluble polysaccharide were purchased from Henan Gaobao Industry Co. (Henan, China). Pepsin (item no. P7125), pancreatin (item no. P7545), and bile salt (item no. 48305) were all purchased from Sigma-Aldrich (Shanghai, China). Solutions were prepared with ultrapure grade water. Growth media, solutions, and glassware were all sterilized by autoclaving at 115 °C for 20 min.

2.2. Bacterial cultivation

The stored LGG cells in a culture tube were transferred onto MRS agar plates, composed of 52 g per L MRS broth powder and 20 g L^{-1} of agar, and incubated at 37 °C for two days before being stored at 4 °C. The culture was refreshed on new agar media weekly to maintain the viability of the LGG. From these plates, a single colony was selected and introduced into sterile MRS broth and then incubated under static conditions at 37 °C for 12 h. This culture was then inoculated into fresh MRS broth, maintaining an added concentration of 2% (v/v). After 24 h in the same environment, the MRS broth was centrifuged at 8000 g for 10 min to collect LGG cells, which reached a density of 1 × 10^9 CFU mL^{-1}. To purify, the cells were washed twice using 0.85% sterile saline under the same centrifugal conditions.

2.3. Spray dying microencapsulation of probiotics

2.3.1. Sample preparation. The samples were prepared in PBS with compositions as shown in Table 1. All liquids were sterilized before spray drying. The activated LGG was inoculated into 50 mL of MRS broth medium at a volume of 2% (v/v) and incubated for 24 h. Cell precipitation was then obtained and mixed with the samples.

2.3.2. Spray drying. Solutions were spray-dried using a spray dryer (Shanghai Pilotech Instrument & Equipment Co., Ltd, China) under the following operating conditions: the inlet temperature was 170 ± 2 °C, while the outlet temperature was 95 ± 5 °C. The feed flow rate was 15 rpm, and the air flow rate was maintained at 30 m^3 h^{-1}. The powder samples were

Table 1 Composition of microcapsules[a]

Composition	L100 (%)	Trehalose (%)	Maltodextrin (%)	Inulin (%)	Soluble soy polysaccharides (%)	Total mass (%)
LT	2	10				12
LT–MD	2	5	5			12
LT–IN	2	5		5		12
LT–SP	2	5			5	12

[a] LT: L100–trehalose; LT–MD: L100–maltodextrin; LT–IN: L100–inulin; LT–SP: L100–soluble soy polysaccharides.

promptly collected and stored in centrifuge tubes for further use.

2.4. Physicochemical properties of spray-dried microcapsules

2.4.1. Water content. The experiment followed the method described by Arepally et al.[19] The moisture content of the powder was determined gravimetrically by drying in an oven at 105 °C until a constant weight was achieved.

2.4.2. Density. The experiment followed the method described by Goula and Adamopoulos.[20] A total of 1–2 g powder was transferred to a 10 mL dry graduated cylinder and weighed on a balance to determine the powder mass. The powder mass was then divided by the volume occupied by the graduated cylinder to calculate the loose bulk density (ρ_b). The measuring cylinder was lifted to a height of 1–2 cm and allowed to drop by itself about 200 times to obtain a certain volume of powder. The powder mass was divided by this volume to determine the trapped bulk density (ρ_t) of the powder.

2.4.3. Hygroscopicity. The hygroscopicity of the powders was evaluated following the method of Paim et al.,[21] with minor modifications. The samples were placed in a flat dish and placed in a desiccator filled with distilled water. The desiccator was sealed with Vaseline and balanced for 24 h to reach $a_w = 1$. At regular intervals, the sample was weighed to determine the amount of water absorbed, and the moisture absorption rate was calculated.

2.4.4. Fourier transform infrared spectroscopy (FT-IR) analysis. A total of 1 mg sample was mixed with 100 mg dried potassium bromide, thoroughly ground under an infrared lamp, and pressed into tablets under a certain pressure for testing. A Fourier transform infrared spectrometer (Antaris™ II, Thermo Fisher, USA) was used to scan and obtain the spectrum. Each test was scanned 64 times with a resolution of 4 cm^{-1} over a scanning range of 400–4000 cm^{-1}.

2.4.5. SEM. The powders were attached to conducting carbon tape fixed on an aluminium stub. The samples were then sputter-coated with gold to enable electrical conductivity and observed under a scanning electron microscope (TM3000, Hitachi, Japan).

2.5. Viable evaluation of LGG after spray drying

The experimental methodology is based on Bhagwat et al.,[22] with minor modifications. The cell viability was determined using the viable cell count method. Briefly, the powder samples were dissolved in 0.05 M PBS (pH 6.5), followed by serial dilutions and plate counting. The encapsulation efficiency was calculated using the following formula:

$$\text{Encapsulation efficiency (\%)} = E/E_0 \times 100 \tag{1}$$

where E_0 refers to the viable cells (CFU mL^{-1}) before drying and E is the viable cells (CFU mL^{-1}) after drying.

2.5.1. Cell re-growth capacity. Powder samples were dissolved in PBS and then added to sterilized liquid MRS with an inoculation volume of 2%. The re-growth curves of spray-dried LGG in different powder samples were characterized by measuring OD 600 and recording their changes at designated time points, followed by data fitting to obtain the final curves.

2.5.2. Cell membrane damage observation. Cell membrane damage was observed using fluorescence staining. The staining used the Syto9/PI live/dead bacterial double stain kit (MX4234-40T; Maokang Biotechnology Co., Ltd, Shanghai, China) and was conducted following the manufacturer's instructions. Briefly, the powder was dissolved and centrifuged to obtain cell precipitation, which was then incubated with Syto9/PI dye in the dark for 15 min. Finally, the samples were observed under a fluorescence microscope at a specific excitation wavelength.

2.6. Cell survival in in vitro digestion

The simulated gastric fluid (SGF) and simulated intestinal fluid (SIF) were prepared according to Minekus et al.[23] with modifications. For SGF, 10 mL was prepared by mixing 0.3 M CaCl$_2$ solution (5 μL), pepsin (50 mg), SGF stock solution (8 mL) and pure water (1.95 mL). The pH of the mixture was adjusted to 2.0. SIF (10 mL) was prepared by combining 0.3 M CaCl$_2$ solution (20 μL), pepsin (125 mg), bile salts (0.08 g), SIF stock solution (8 mL) and pure water (1.95 mL), with the final pH adjusted to 7.0.

To conduct the experiment, a mixture of 10 mL of SGF and 0.1 g of spray-dried powder was prepared. Before digestion, the pH of the solution was readjusted to 2.0. The mixture was then subjected to water bath oscillation for 2 h at 37 °C and 50 rpm. Subsequently, 10 mL of SIF was added to the gastric fluid mixture, and the pH of the digestion juice was adjusted to 7.0 before incubating for another 2 h under the same conditions. Samples of 500 μL were collected at 0, 1, 2, 3, and 4 h during continuous digestion. The samples obtained at each time point were diluted and spread onto MRS agar plates for static incubation at 37 °C for 48 h to detect bacterial viability.

2.7. Cell survival during storage

The spray-dried powders were stored in hermetically sealed tubes at 4 ± 1 °C, and the number of viable cells was detected weekly.

2.8. Adhesion to Caco-2 monolayer cells

2.8.1. Cell culture. The experimental method is based on Golowczyc et al.,[24] with minor modifications. A Caco-2 cell tube was removed from the liquid nitrogen tank, and the cell suspension rapidly thawed in a 37 °C water bath before being transferred to a sterile centrifuge tube. To minimize damage from the frozen solution to the cells, 1 mL of complete cell culture medium (composed of 80% (v/v) DMEM, 20% (v/v) fetal bovine serum, and 1% (v/v) dual antibody) was added. After low-speed centrifugation (500 rcf, 5 min), the supernatant was discarded, and 5 mL of cell culture medium was added to resuspend the cell precipitate. The cell suspension was then inoculated into a T25 culture bottle and incubated at 37 °C and 5% CO_2. The medium was changed the following day, and passage was performed when the cell density reached 80–90%.

For passage, the cell monolayer was washed with PBS, and 0.5 mL of trypsin–EDTA solution was added for digestion until the cell monolayer was detached into individual cells. Subsequently, 0.5 mL of cell culture medium was added to terminate digestion. The obtained cell suspension was transferred to a sterile centrifuge tube for centrifugation, resuspended in culture medium, and then passaged at a ratio of 1 : 2.

2.8.2. Adhesion rate. After the cells inoculated in T25 grew for 2–3 days and reached a density of 80–90%, the tight junction protein between cells was digested using trypsin–EDTA digestion solution. After centrifugation at low speed, the supernatant was discarded, and the cells were resuspended in complete culture medium. Subsequently, the cell suspension was inoculated into a 12-well plate with a volume of 50 000 cells per well and cultured for 2–3 days for the experiment.

The monolayer was used for the evaluation tests of bacterial adhesion ability, following the method described by Xu et al.[25] with some modifications. Firstly, cells were collected and resuspended in PBS. After incubation at 37 °C for 2 h, the cells were washed three times with sterile PBS to remove free cells. Next, 0.5 mL trypsin was added to disrupt the monolayer, followed by incubation at 37 °C for 7 min. Finally, 0.5 mL medium was added to deactivate the trypsin. The mixture was then serially diluted for plate colony counting in a centrifuge tube as proposed previously. The viable cells were detected before the Caco-2 adhesion tests. The adhesion rate was expressed as below:

$$\text{Adhesion rate } (\%) = N/N_0 \qquad (2)$$

where N is the number of viable cells after the adhesion test, and N_0 is the number of viable cells before the adhesion test.

2.8.3. Adhesion observation. Cells were cultivated in a 12-well plate using the same method. Before inoculation, tissue culture-treated glass slides were placed in the plate for subsequent observation. The LGG cells were stained with CFDA-SE (5(6)-carboxyfluorescein diacetate succinimidyl ester) at a final

concentration of 20 µM. After incubation in the dark for 15 min, the LGG cells were labelled, and the residual dyes were finally washed away by multiple rounds of centrifugation. The LGG cells, with a density of 10^7 CFU mL^{-1}, were finally resuspended in sterile PBS. The medium in the 12-well plate was discarded, and 1 mL of DMEM medium was added to each well, followed by the addition of 0.5 mL of LGG cell suspension. The plate was then incubated at 37 °C for 2 h. After incubation, the 12-well plate was washed three times with sterile PBS and then incubated with 4% paraformaldehyde for 15 min to fix the cells. The slides were taken out and placed on the other slides to observe under a laser confocal microscope (TCS SP8 X, Leika, German).

2.9. Statistical analysis

All experiments and analyses were conducted in triplicate. The results were expressed as means ± standard deviation (SD), and data analysis was performed using SPSS software (version 26, SPSS Inc., Chicago, USA) with one-way ANOVA ($p < 0.05$) for statistical significance.

3. Results and discussion

3.1. Physicochemical properties of L100–Tre–LGG based microcapsules

All powders obtained through spray drying were similar in colour, with the LT–SP powder appearing light yellow due to the presence of SSP (Fig. 1a).

3.1.1. Water content. The moisture content of the four powders was between 4.84 and 6.22% (Table 2), with a significant difference between samples. Among them, the LT powder had the lowest moisture content, while the LT–SP powder had the highest. This is consistent with a previous study conducted by Huang et al.,[26] which found that the water content of concentrated whey protein probiotic spray-dried powder ranged between 5% and 6%. Generally, foods with lower moisture content are more stable during storage.[27] The moisture content of particles is closely related to drying parameters. Higher inlet temperatures can reduce the moisture content of the powder but may exacerbate damage to probiotics. In contrast, lower inlet temperature can increase powder moisture content, which can negatively affect the storage stability of products.[28,29]

3.1.2. Density. As shown in Table 2, the statistical analysis revealed no significant difference in the ρ_b of all powders ($p > 0.05$), whereas a significant difference was observed in ρ_t ($p < 0.05$). Among the powders, LT–SP exhibited the highest ρ_t, while LT–IN showed the lowest. The bulk density of a powder is influenced to a certain extent by particle size and morphology. Typically, smaller particle sizes lead to higher ρ_b.[30] The ρ_t serves as an indicator of the transportation convenience of powder products. A higher ρ_t results in a smaller packaging size required for transportation and storage, which facilitates ease of handling and transportation.[31] Moreover, the density of the powder can influence the interactions between particles, such as friction and collision. A higher density tends to increase these interactions, thereby affecting the looseness and flow rate of the powder.
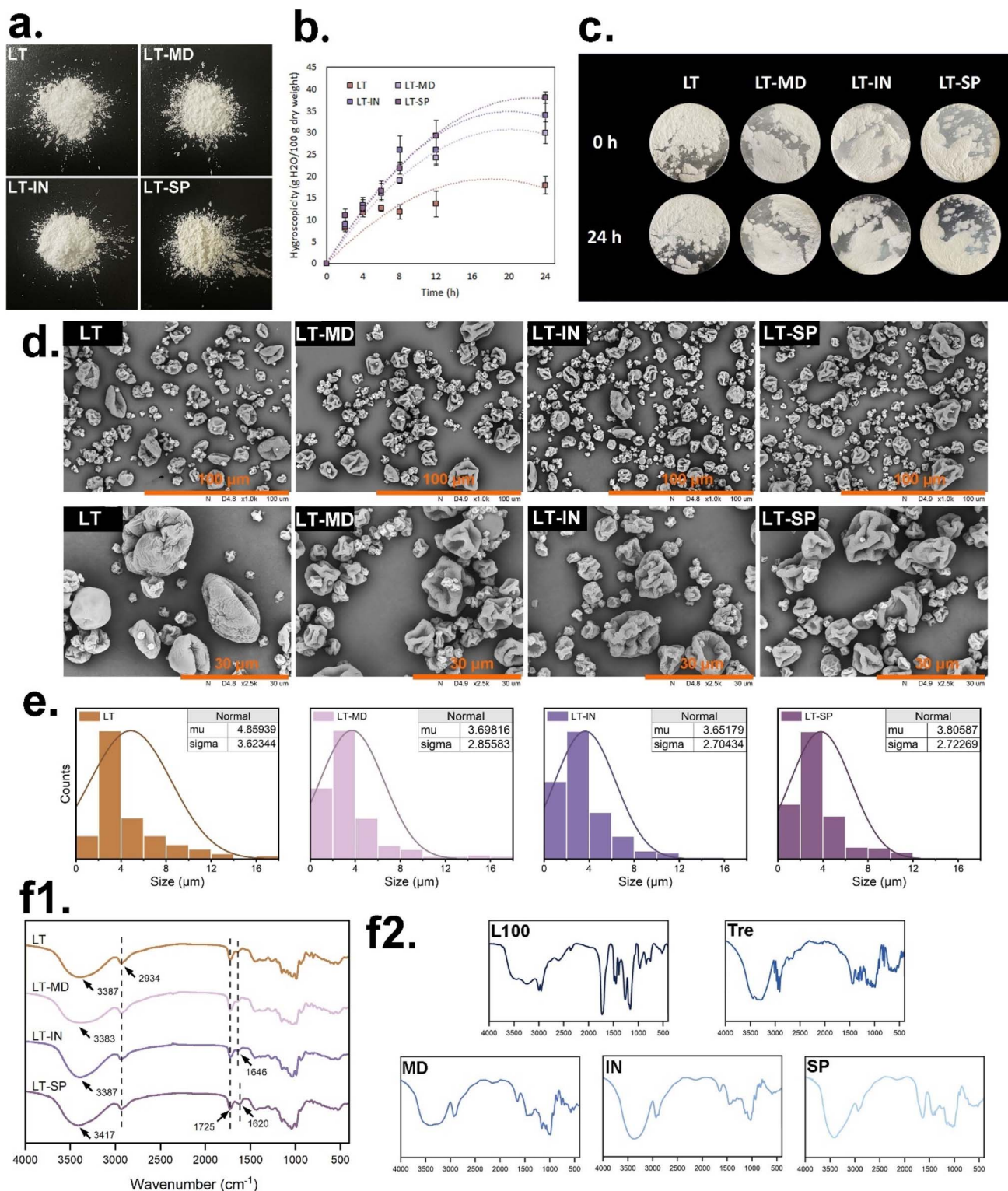
Fig. 1 (a) The appearance of spray-dried powders; (b) hygroscopicity of powders; (c) comparison of powder moisture absorption before and after 24 h; (d) microstructure of particles captured using an SEM; (e) size distribution of powders; (f) FT-IR spectrum of spray-dried powders (f1) and wall materials (f2).

3.1.3. Hygroscopicity. Hygroscopicity is a crucial parameter in evaluating the stability of powder storage. Fig. 1b and c show the hygroscopic behaviours of the powders in an environment with $a_w = 1$, along with the powder's morphological changes before and after exposure to moisture. Comparing the moisture absorptions of the four powders before and after 24 h, it is evident that all four powders underwent agglomeration and adhesion. Notably, the LT powder exhibited the lowest moisture

Table 2 Physicochemical properties of powders[a]

Properties	LT	LT–MD	LT–IN	LT–SP
Moisture content (%)	4.84 ± 0.59^a	6.02 ± 0.38^{ab}	5.37 ± 0.56^{ab}	6.22 ± 0.34^b
ρ_t (g mL^{-1})	0.29 ± 0.04^{ab}	0.27 ± 0.003^a	0.26 ± 0.03^a	0.34 ± 0.003^b
ρ_b (g mL^{-1})	0.41 ± 0.07^a	0.48 ± 0.04^a	0.51 ± 0.09^a	0.57 ± 0.05^a

[a] Values followed by the different superscript letters in the same row are significantly different ($p < 0.05$).

absorption rate, accounting for 17.94% weight gain, whereas the LT–SP powder showed the highest moisture absorption rate, reaching 38.04%.

The moisture absorption ability of a powder is closely linked to the interaction between its wall material and water molecules. Compared with LT powders, LT–MD, LT–IN, and LT–SP powders exhibited higher water absorption rates. This enhanced absorption can be attributed to the abundance of hydroxyl groups in polysaccharides, which facilitate stronger bonding with water molecules.[32] In fact, for powder products, a high moisture absorption rate indicates that the sample is more prone to attracting moisture from the surrounding environment. This, in turn, can negatively impact the storage stability and powder flowability, potentially leading to adhesion and clumping during the shelf life. Moreover, water absorbed from the external environment can accelerate redox reactions within the particles, thereby affecting their biological activity.[20] Therefore, controlling the moisture absorption rate is crucial for ensuring the stability, flowability, and bioactivity of powder products.

3.1.4. Morphology. As shown in Fig. 1d, the surface morphology of the four powders displayed distinct indentations. These indentations were mainly attributed to the rapid evaporation of water during the drying process.[33] Interestingly, the LT–MD, LT–IN, and LT–SP particles exhibited more pronounced wrinkled surfaces compared to the LT powder. The addition of polysaccharides appears to intensify this wrinkled morphology on the particle surface. In contrast, the morphology of the LT powder is similar to the particle shape achieved through single droplet drying, showing a bowl-like shape with a relatively smooth surface.[18] It is worth noting that no obvious cracks were observed on the surfaces of all four powders, suggesting their ability to provide a robust environmental barrier for the encapsulated LGG.[34] This feature is crucial for maintaining the viability and stability of the encapsulated bacteria. With regard to particle size, all four powders exhibited an average particle diameter below 5 μm (Fig. 1e). Among them, the LT powder showed the largest particle size, with a value of 4.86 μm. Particle size is a crucial parameter influencing the flowability of powders, as larger particles tend to have greater interstitial spaces between them, facilitating particle flow.

3.1.5. FT-IR spectra analysis. The spectra of the four spray-dried microcapsules were similar (Fig. 1f1), indicating a prevalence of common sugar structures across the samples. These included –OH and glycosidic bonds. Minor variations in the –OH peaks were observed among the different samples. The peaks for the LT, LT–MD, and LT–IN microcapsules were located at 3387 cm^{-1} or 3383 cm^{-1}, while the TL-ST microcapsules displayed a –OH peak at 3417 cm^{-1}. The absorption band observed at 2934 cm^{-1} corresponded to the stretching vibration of the –CH group in alkanes, while the absorption band at 1725 cm^{-1} was a characteristic peak associated with the carbonyl groups present in L100.[35] The absorption bands located at 1646 cm^{-1} in the spectra of LT, LT–MD and LT–IN and at 1620 cm^{-1} in the LT–SP spectrum represented the presence of 1,4-β glycoside bonds. A comparison with the spectral diagram of the wall material (Fig. 1f2) reveals that the functional groups and chemical bonds of these compounds remained largely unchanged after spray drying.[36] This indicated that the chemical integrity of the compounds was successfully preserved.

3.2. The viability and adhesion activity of cells in L100–Tre based spray-dried powders

3.2.1. The viable cell numbers and encapsulation efficiency of LGG. As shown in Fig. 2a, after spray drying, the viable counts of LGG in LT, LT–MD, LT–IN, and LT–SP powders were higher than 9 log CFU g^{-1}. Notably, the retention of live bacteria in LT and LT–SP samples was significantly higher ($p > 0.05$) than in the other two samples. The results showed that the microcapsules exhibited high resistance to spray drying stress, which verified the effectiveness of the encapsulation system in protecting LGG viability. Meanwhile, the encapsulation efficiency of the four powders was in accordance with the cell viability retention as expected. It is believed that sugars can stabilize cell membranes through hydrogen bonding, effectively preventing hydrogen protons from easily entering cells, thereby maintaining pH equilibrium within and outside the cells. This mechanism played a pivotal role in protecting probiotics from environmental stress.[37] In contrast, although MD, IN and SP offered some protective effects, their ability to protect probiotics during spray drying was not as good as that of Tre. This disparity was mainly because the steric hindrance effect of polysaccharides was relatively low, which made them less effective in preventing cell damage compared to Tre.[38] Therefore, when selecting wall materials, it is necessary to comprehensively consider their probiotic protective ability and practical application requirements.

3.2.2. The re-growth capability of LGG after spray drying. The re-growth curves of spray-dried LGG cells in the four powder samples, as shown in Fig. 2b, provide further confirmation of the cell damage during the spray drying process. Compared to LGG cells that were not subjected to spray drying, the logarithmic growth phase of the spray-dried cells was significantly delayed, which was probably due to a decrease in viable cell counts within the microcapsules and subcellular damage to the cells.[39] Among the four samples, the LT–MD powder exhibited the most pronounced cell growth lag,
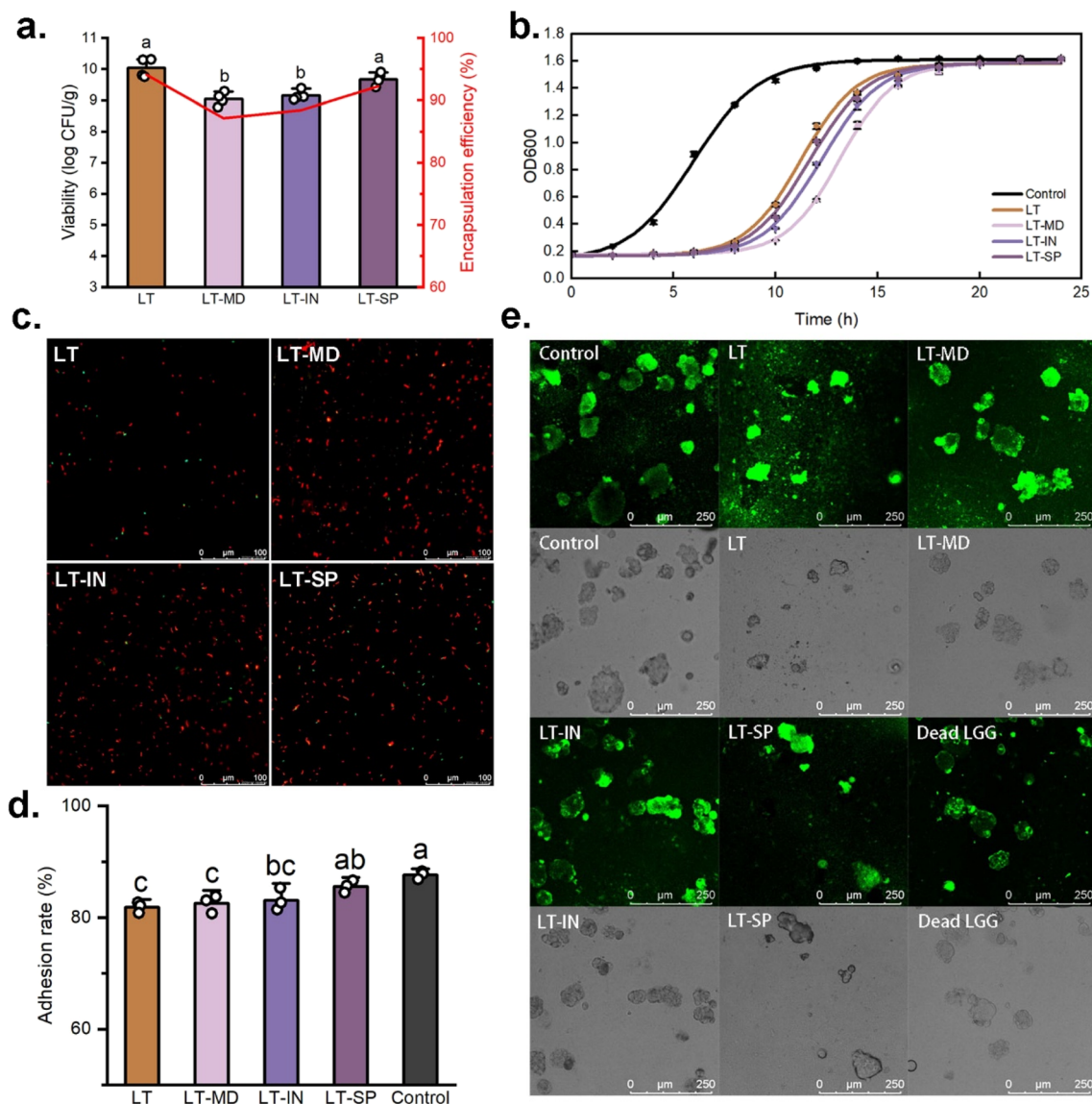
Fig. 2 (a) Viable cell numbers and encapsulation efficiency of LGG; (b) growth curve of LGG after spray drying; (c) fluorescence staining images of LGG in powder; (d) adhesion capacity of LGG to cells after spray drying; (e) fluorescence staining images of LGG adhered to Caco-2 cells (lethal LGG by heat treatment).

indicating the most severe subcellular damage to the cells in this sample. However, once the cell growth entered a stable phase, the growth curves of the LGG in all four samples closely aligned with those of non-spray-dried LGG, suggesting that despite spray drying, the cells retained good reproductive capacity.[39,40] This finding indicated that the L100–Tre or L100–Tre–polysaccharide encapsulation system offered a protective effect to the LGG during the drying process, enabling them to maintain good growth potential after spray drying.

3.2.3. Membrane integrity of LGG after spray drying. As shown in Fig. 2c, cells with intact cell membranes exhibit green fluorescence, while damaged membranes emit red fluorescence due to binding with PI dyes. The LT sample displayed the highest ratio of green fluorescent spots, indicating superior integrity of its cell membranes. This finding was supported by the results shown in Fig. 2a and b. In contrast, the LT–SP, LT–IN, and LT–MD

samples exhibited a marked decrease in green fluorescence, particularly in the LT–MD sample, where green fluorescence was nearly undetectable. This reduction was attributed to the increased number of damaged cells in these samples, where the intense red fluorescence obscured the green fluorescence. Cell membrane damage, a major cause of cell death during spray drying, increases membrane permeability, allowing non-selective entry of extracellular components, ultimately leading to cell death.[7] Thus, optimizing spray drying conditions and selecting suitable carriers are essential for protecting the integrity of probiotic cell membranes.

3.2.4. Adhesion ability of LGG after spray drying. In this study, the Caco-2 cell monolayer model served as a model for the human intestinal environment to evaluate the impact of spray drying microencapsulation on the adhesion of LGG under various encapsulation systems. Caco-2 cells, a widely employed intestinal cell line, mimic the structure and function of differentiated small

intestinal epithelial cells, including microvilli and enzyme systems similar to the brush border epithelium of the small intestine.[41] As shown in Fig. 2d, spray drying microencapsulation had a minimal influence on the adhesion of LGG. Generally, the adhesion rate of spray-dried LGG remained above 80%, indicating a high adhesive ability.[42] Among them, the adhesion level of LGG encapsulated in LT–SP powder was comparable to that of untreated LGG, and the adhesion capacity of LGG in LT, LT–MD, and LT–IN powders was also similar. An excellent encapsulation system could be a contributing factor to LGG's ability to maintain a high adhesion rate. The wall material protects the integrity of LGG's cell structure, including the surface protein receptor and pili, during spray drying, thereby enabling it to effectively adhere to the Caco-2 monolayer.[43]

Consistent findings were observed in the adhesion analysis (Fig. 2e). LGG labelled with CFDA-SE adhered to the surface of Caco-2 cells, emitting green fluorescence. Notably, even after high-temperature inactivation, LGG was still able to adhere to Caco-2 cells, though its distribution was less uniform compared to live cells. This may be due to the spontaneous absorption of LGG aggregates by Caco-2 cells. Similar studies have also shown that *Lactobacillus acidophilus*, following heat treatment at 100–105 °C, can adhere to HeLa 299 cells and inhibit the adhesion of *Escherichia* coli B41.[44] This suggested that even after high-temperature treatment, the surface of LGG cells retained molecular structures that can be recognized by Caco-2 cells.

Golowczyc et al.[24] found that spray drying did not significantly alter the adhesion function of *Lactobacillus plantarum* 83114 and *Lactobacillus kefir* 8321, but it significantly reduced the adhesion ability of *Lactobacillus kefir* 8348. This underlines the strain-specific effect of spray drying on bacterial adhesion, as previously reported by Iaconelli et al.[45] Therefore, when producing probiotic powders using spray drying, it is crucial to comprehensively evaluate its potential impacts on the specific functionalities of the target strain to ensure optimal performance.

3.3. The stability of cell viability

3.3.1. The stability of cell viability in spray-dried powders during *in vitro* digestion. As shown in Fig. 3a, LGG showed varied losses in viability after simulated gastrointestinal digestion. Specifically, although encapsulated by composite wall materials containing L100, the LGG cells within the microcapsules still experienced a viability reduction of 7–13% after 2 h of simulated gastric digestion. Among the samples, LT particles showed the highest bacterial viability retention rate, reaching 93%, while LT–SP samples exhibited the lowest retention rate at 87.4%. This variation could be due to the fact that some digestive fluid infiltrated into the interior of the particles through small channels or defects on the surface during the simulated gastric digestion, allowing direct contact with LGG cells, thus causing damage or inactivation of the probiotic cells.[18]

During the simulated intestinal digestion, the bacterial cells encapsulated within the particles were released and had to face the stressful conditions of bile salts and pancreatic enzymes.[46] Although no significant difference ($p > 0.05$) in bacterial viability was observed among the four powders after spray drying, significant variations ($p < 0.05$) in viability were observed after 4 h of simulated gastrointestinal digestion. The results indicated that probiotics encapsulated with IN or SP were more sensitive to these stresses. Specifically, after 4 h of digestion, the bacterial viability levels in LT–IN and LT–SP powders decreased to 83.6% and 78%, respectively, while LT powder maintained the highest viability retention at 91.2%. This may be attributed to the more severe damage inflicted on the cells during spray drying in LT–IN and LT–SP powders, making them more vulnerable to the stress of bile salts and trypsin presented in the SIF. Gonzalez-Ferrero et al.[47] also emphasized the challenging gut environment for probiotics, discovering that probiotics encapsulated with soy protein concentrate and maltodextrin showed minimal viability loss in SGF but substantial cell death in SIF.

Overall, after 4 h of simulated *in vitro* digestion, the survival rates of spray-dried LGG in all powders were above 78%, indicating that MD, IN, and SP exhibited certain protective effects during the *in vitro* digestion of LGG. These findings align with similar studies that have reported the good resistance of probiotics encapsulated in IN and MD against low pH and bile stress.[36] These results provide insights into the protective effects
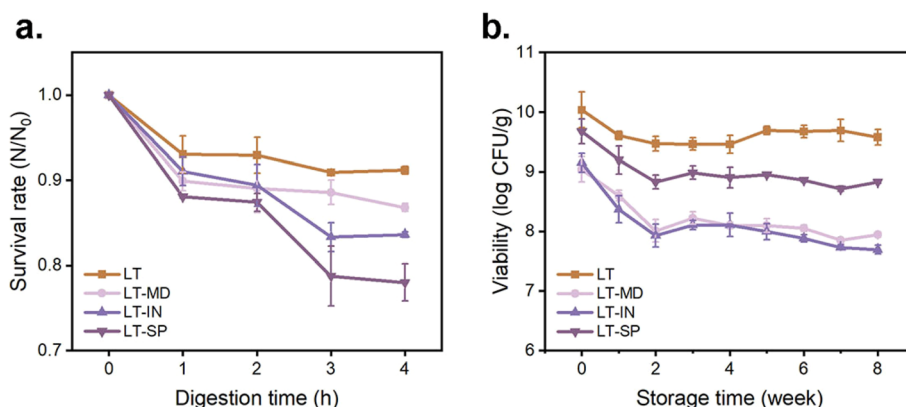

Fig. 3 Digestion and storage stability. (a) survival rate of cells in microcapsules after simulated *in vitro* digestion. (b) Viability of cells in microcapsules stored at 4 °C.

of different wall materials for probiotics in simulated digestive environments, which can help optimize the formulation and stability of probiotic products.

3.3.2. The stability of cell viability in spray-dried powders during storage.

As shown in Fig. 3b, after 8 weeks of storage, the viability of LGG encapsulated in the four microcapsules showed varying degrees of loss. Among them, LT–MD and LT–IN showed significant viability reductions, with decreases of 12.2% and 16%, respectively. In contrast, probiotics in LT powder showed minimal viability loss, with only a decrease of 4.6%. However, all four microcapsules maintained a probiotic viability above 7 log CFU g^{-1} after 8 weeks of storage, demonstrating desirable storage stability. This can be attributed to the high glass transition temperature of Tre, which acted as an efficient protective agent for bacterial cells. Tre can effectively protect probiotic cells from environmental pressures, preserving cell integrity and viability.[33] In addition, Tre bound with water molecules on the cell surface, forming a protective film that further enhanced the storage stability of probiotics. These findings were consistent with the study conducted by Nunes et al.,[48] who reported that *Lactobacillus* La-5 encapsulated in Tre maintained robust viability even after 120 days of storage at varying temperatures. Similarly, Zhang et al.[49] reported that *Lactobacillus salivarius* NRRL B-30514 encapsulated with Tre and skimmed milk showed better survival during storage than powder produced with skimmed milk only.

It is worth noting that for the four microcapsules, LGG experienced a distinct loss of viability during the initial storage period, and then the viability began to regain, followed by a slower rate of bacterial viability loss (Fig. 3b). This pattern of viability fluctuation has been similarly observed in the study conducted by Reyes et al.[50] This phenomenon could be due to the environmental pressure encountered by the bacterial cells upon storage. However, as the storage period progressed, some bacterial cells gradually adapted to these conditions and began to regain viability through their inherent repair mechanisms. In addition, the refrigeration conditions used for storage likely contributed to the improved stability of the cells, potentially by reducing harmful chemical reactions like redox reactions. This finding is consistent with the observations made by Broeckx et al.,[51] further confirming the importance of refrigeration in preserving probiotic viability during storage.

4. Conclusion

In this study, we successfully fabricated L100–Tre–LGG microcapsules using a spray drying technique and analysed the physicochemical properties of the resulting powders containing L100–Tre and polysaccharides. The results revealed that the particles exhibited good physicochemical characteristics, and the encapsulated LGG showed desirable viability, re-growth capability, and storage stability. Furthermore, the spray-dried LGG in the L100–Tre-based microcapsules maintained high viability during simulated *in vitro* digestion, confirming their high digestive stability. In addition, the study investigated the adhesion functionality of the LGG encapsulated in the L100–Tre-based microcapsules and found that the spray drying process had a limited impact on the

bacterial adhesion capacity. Overall, these findings demonstrated the high viability retention and adhesion capacities of the L100–Tre–LGG probiotic spray-dried particles, providing strong support for the development and application of spray-dried probiotic powder products.

Data availability

The data supporting this paper have been included in the paper.

Conflicts of interest

On behalf of all the authors, the corresponding author states that there is no conflict of interest.

Acknowledgements

References

1 C. Hill, F. Guarner, G. Reid, G. R. Gibson, D. J. Merenstein, B. Pot, L. Morelli, R. B. Canani, H. J. Flint, S. Salminen, P. C. Calder and M. E. Sanders, *Nat. Rev. Gastroenterol. Hepatol.*, 2014, **11**, 506–514.

2 J. F. Cryan, K. J. O'Riordan, C. S. M. Cowan, K. V. Sandhu, T. F. S. Bastiaanssen, M. Boehme, M. G. Codagnone, S. Cussotto, C. Fulling, A. V. Golubeva, K. E. Guzzetta, M. Jaggar, C. M. Long-Smith, J. M. Lyte, J. A. Martin, A. Molinero-Perez, G. Moloney, E. Morelli, E. Morillas, R. O'Connor, J. S. Cruz-Pereira, V. L. Peterson, K. Rea, N. L. Ritz, E. Sherwin, S. Spichak, E. M. Teichman, M. van de Wouw, A. P. Ventura-Silva, S. E. Wallace-Fitzsimons, N. Hyland, G. Clarke and T. G. Dinan, *Physiol. Rev.*, 2019, **99**, 1877–2013.

3 G. Sharon, N. J. Cruz, D. W. Kang, M. J. Gandal, B. Wang, Y. M. Kim, E. M. Zink, C. P. Casey, B. C. Taylor, C. J. Lane, L. M. Bramer, N. G. Isern, D. W. Hoyt, C. Noecker, M. J. Sweredoski, A. Moradian, E. Borenstein, J. K. Jansson, R. Knight, T. O. Metz, C. Lois, D. H. Geschwind, R. Krajmalnik-Brown and S. K. Mazmanian, *Cell*, 2019, **177**, 1600–1618.

4 A. Rivière, M. Selak, D. Lantin, F. Leroy and L. De Vuyst, *Front. Microbiol.*, 2016, **7**, 979.

5 A. L. Servin, *FEMS Microbiol. Rev.*, 2004, **28**, 405–440.

6 S. Huang, M. L. Vignolles, X. D. Chen, Y. Le Loir, G. Jan, P. Schuck and R. Jeantet, *Trends Food Sci. Technol.*, 2017, **63**, 1–17.

7 E. Ananta, M. Volkert and D. Knorr, *Int. Dairy J.*, 2005, **15**, 399–409.

8 P. Teixeira, H. Castro, C. Mohácsi-Farkas and R. Kirby, *J. Appl. Microbiol.*, 1997, **83**, 219–226.

9 C. Santivarangkna, M. Wenning, P. Foerst and U. Kulozik, *J. Appl. Microbiol.*, 2007, **102**, 748–756.

10 C. Santivarangkna, U. Kulozik and P. Foerst, *J. Appl. Microbiol.*, 2008, **105**, 1–13.

11 L. K. Liao, X. Y. Wei, X. Gong, J. H. Li, T. Huang and T. Xiong, *LWT–Food Sci. Technol.*, 2017, **82**, 82–89.

12 Z. Muhammad, R. Ramzan, R. F. Zhang and M. W. Zhang, *Coatings*, 2021, **11**, 587.

13 Y. Xu, M. Dong, H. Xiao, S. Y. Quek, Y. Ogawa, G. Ma and C. Zhang, *Crit. Rev. Food Sci. Nutr.*, 2023, 1–17.

14 O. Alvarado-Reveles, S. Fernandez-Michel, R. Jimenez-Flores, C. Cueto-Wong, L. Vazquez-Moreno and G. R. C. Montfort, *Probiotics Antimicrob. Proteins*, 2019, **11**, 1340–1347.

15 P. Chaikham, V. Kemsawasd and P. Seesuriyachan, *LWT*, 2017, **78**, 31–40.

16 Y. Xu, D. Mingsheng, X. Hongmei, Y. Q. Siew, O. Yukiharu, M. Guangyuan and C. and Zhang, *Crit. Rev. Food Sci. Nutr.*, 2024, **64**, 11222–11238.

17 S. S. Pinto, S. Verruck, C. R. W. Vieira, E. S. Prudêncio, E. R. Amante and R. D. M. C. Amboni, *LWT–Food Sci. Technol.*, 2015, **64**, 1004–1009.

18 Y. Xu, S. Zhu, Y. Zeng, C. Zhang, M. Dong and C. Zhang, *J. Food Eng.*, 2024, **369**, 111940.

19 D. Arepally, R. S. Reddy and T. K. Goswami, *Food Funct.*, 2020, **11**, 8694–8706.

20 A. M. Goula and K. G. Adamopoulos, *Drying Technol.*, 2008, **26**, 726–737.

21 D. Paim, S. D. O. Costa, E. H. M. Walter and R. V. Tonon, *LWT–Food Sci. Technol.*, 2016, **74**, 21–25.

22 A. Bhagwat, P. Bhushette and U. S. Annapure, *Beni-Suef Univ. J. Basic Appl. Sci.*, 2020, **9**, 1–8.

23 M. Minekus, M. Alminger, P. Alvito, S. Ballance, T. Bohn, C. Bourlieu, F. Carriere, R. Boutrou, M. Corredig, D. Dupont, C. Dufour, L. Egger, M. Golding, S. Karakaya, B. Kirkhus, S. Le Feunteun, U. Lesmes, A. Macierzanka, A. Mackie, S. Marze, D. J. McClements, O. Menard, I. Recio, C. N. Santos, R. P. Singh, G. E. Vegarud, M. S. Wickham, W. Weitschies and A. Brodkorb, *Food Funct.*, 2014, **5**, 1113–1124.

24 M. A. Golowczyc, P. T. JoanaSilva, G. L. D. Antoni and A. G. Abraham, *Int. J. Food Microbiol.*, 2011, **144**, 556–560.

25 D. Xu, X. Zhao, G. C. Mahsa, K. Ma, C. Zhang, X. Rui, M. Dong and W. Li, *Carbohydr. Polym.*, 2023, **313**, 120874.

26 S. Huang, S. Mejean, H. Rabah, A. Dolivet, Y. Le Loir, X. D. Chen, G. Jan, R. Jeantet and P. Schuck, *J. Food Eng.*, 2017, **196**, 11–17.

27 P. Vaibhav, K. C. Anil and P. S. Surendra, *Int. J. Curr. Microbiol. Appl. Sci.*, 2014, **3**, 1224–1237.

28 D. Arepally and T. K. Goswami, *LWT–Food Sci. Technol.*, 2019, **99**, 583–593.

29 A. Rodklongtan and P. Chitprasert, *Food Res. Int.*, 2017, **100**, 276–283.

30 M. F. Zotarelli, V. M. da Silva, A. Durigon, M. D. Hubinger and J. B. Laurindo, *Powder Technol.*, 2017, **305**, 447–454.

31 S. George, A. Thomas, M. V. P. Kumar, A. S. Kamdod, A. Rajput, T. J. Joshi and S. Abdullah, *Eur. Food Res. Technol.*, 2023, **249**, 241–257.

32 C. Zhang, S. L. Ada Khoo, X. D. Chen and S. Y. Quek, *Powder Technol.*, 2020, **361**, 995–1005.

33 P. Barajas-Alvarez, M. Gonzalez-Avila and H. Espinosa-Andrews, *LWT–Food Sci. Technol.*, 2022, **153**, 112485.

34 R. Rajam and C. Anandharamakrishnan, *LWT–Food Sci. Technol.*, 2015, **60**, 773–780.

35 S. Thakral, N. K. Thakral and D. K. Majumdar, *Expert Opin. Drug Delivery*, 2013, **10**, 131–149.

36 V. Kumar, J. J. Ahire, R. Amrutha, S. Nain and N. K. Taneja, *Probiotics Antimicrob. Proteins*, 2023, 10115.

37 R. M. Wang, N. Li, K. Zheng and J. F. Hao, *FEMS Microbiol. Lett.*, 2018, **365**, fny217.

38 P. Jayaprakash, C. Gaiani, J.-M. Edorh, F. Borges, E. Beaupeux, A. Maudhuit and S. Desobry, *Foods*, 2023, **12**, 3117.

39 M. Yin, M. Chen, Y. Yuan, F. Liu and F. Zhong, *Food Hydrocoll.*, 2024, **146**, 109252.

40 Y. Luo, Z. Ma, C. De Souza, S. Wang, F. Qiao, H. Yi, P. Gong, Z. Zhang, T. Liu, L. Zhang and K. Lin, *Food Hydrocoll.*, 2024, **149**, 109602.

41 M. L. Van Tassell and M. J. Miller, *Nutrients*, 2011, **3**, 613–636.

42 B. Sophatha, S. Piwat and R. Teanpaisan, *Arch. Microbiol.*, 2020, **202**, 1349–1357.

43 S. Lebeer, I. Claes, H. L. P. Tytgat, T. L. A. Verhoeven, E. Marien, I. von Ossowski, J. Reunanen, A. Palva, W. M. de Vos, S. C. J. De Keersmaecker and J. Vanderleyden, *Appl. Environ. Microbiol.*, 2012, **78**, 185–193.

44 J. Fourniat, C. Colomban, C. Linxe and D. Karam, *Ann. Rech. Vet.*, 1992, **23**, 361–370.

45 C. Iaconelli, G. Lemetais, N. Kechaouc, F. Chain, L. G. Bermudez-Humaran, P. Langella, P. Gervais and L. Beney, *J. Biotechnol.*, 2015, **214**, 17–26.

46 R. Arevalo-Perez, C. Maderuelo and J. M. Lanao, *J. Controlled Release*, 2020, **327**, 703–724.

47 C. Gonzalez-Ferrero, J. M. Irache and C. J. Gonzalez-Navarro, *Food Chem.*, 2018, **239**, 879–888.

48 G. L. Nunes, M. D. Etchepare, A. J. Cichoski, L. Q. Zepka, E. J. Lopes, J. S. Barin, E. M. D. Flores, C. D. da Silva and C. R. de Menezes, *LWT–Food Sci. Technol.*, 2018, **89**, 128–133.

49 Y. Zhang, J. Lin and Q. X. Zhong, *Food Res. Int.*, 2015, **71**, 9–15.

50 V. Reyes, A. Chotiko, A. Chouljenko, V. Campbell, C. Liu, C. Theegala and S. Sathivel, *Drying Technol.*, 2018, **36**, 1738–1748.

51 G. Broeckx, D. Vandenheuvel, T. Henkens, S. Kiekens, M. F. L. van den Broek, S. Lebeer and F. Kiekens, *Int. J. Pharm.*, 2017, **534**, 35–41.